Int. J. Electrochem. Sci., 10 **(2015)** 1616 - 1631

International Journal of
ELECTROCHEMICAL
SCIENCE
www.electrochemsci.org

Electrochemical Corrosion Characteristics of Super Duplex Stainless Steel S32750 in LT-MED Environment

Huabing Li[1,*], *Zhouhua Jiang*[1,*], *Hao Feng*[1], *Qi Wang*[1], *Wei Zhang*[2], *Guangwei Fan*[2], *Guoping Li*[2], *Leiying Wang*[3]

[1]School of Materials and Metallurgy, Northeastern University, Shenyang 110819, China
[2]Technology Center of Taiyuan Iron and Steel Group Co.Ltd, Taiyuan 030003, China
[3]Technology Center of Xining Special Steel Co. Ltd, Xining 810005, China
[*]E-mail: lihb@smm.neu.edu.cn; Jiangzh@smm.neu.edu.cn

Received: 8 November 2014 / *Accepted:* 16 December 2014 / *Published:* 30 December 2014

The electrochemical corrosion characteristics of super duplex stainless steel S32750 in LT-MED environment was carried out to investigate the effect of seawater temperature and concentration on the corrosion resistance and protective properties of the passive films using different electrochemical techniques. The results the pitting corrosion potential decreases, the passivity current density increases, induction period of pitting shortens and passivation index *n* decreases with the increase of temperature and seawater concentration. E_b - E_p values and the area of hysteresis loop become larger with higher temperature and seawater concentration, indicating the pitting susceptibility of passive films increases. EIS reveals that impedance decreases with increasing seawater temperature and concentration, and the protective ability is provided by the inner oxide layer, while the outer film is more defective. Mott-Schottky analysis shows that passive film present bilayer structure, and behaves as n-type and p-type, respectively. The donor and acceptor densities increase with seawater temperature and concentration, revealing passive films become more defective, resulting in decreasing of protective ability of the passive films.

Keywords: Super Duplex Stainless Steel, LT-MED, Electrochemical Corrosion Characteristics, Seawater Temperature and Concentration, Passive Films

1. INTRODUCTION

Due to rapid population growth, increasing urbanisation and farming, there will be a growing shortage of fresh water all over the world. Available fresh water only accounts for less than 0.5% of the earth's total water supply[1]. A lack of fresh water will put pressure on food prices, constrain developing countries' poverty reduction efforts and hamper economic growth. Incremental technology

as an open source of water, desalination has become an important way to solve the global water crisis. Low Temperature Multi Effect Distillation (LT-MED) is one of the most efficient thermal desalination processes currently in use. Some LT-MED plants usually operate at a maximum brine temperature of 70°C and water concentration ratio of no more than two times [2], which reduces the potential for scale formation and corrosion issues. Due to the high salinity, strong conductivity and large biological activity of seawater, the desalination process is often accompanied by heat or pressure conditions, the corrosion law of material in seawater environment in different regions vary greatly [3]. Furthermore, with the application and development of LT-MED technology, there exists an increasing need of higher temperature and brine concentration in the desalinators to reduce the drainage of hot brine and increase the water production ratio [4,5]. Thus for more aggressive chloride attack and higher temperature, the material used in LT-MED environment with excellent corrosion resistance and higher strength must be needed. The 316L and 317L stainless steels are often used as evaporation chambers material, but pitting and crevice corrosion occur frequently when the material is long-term immersed in seawater [6]. Copper-nickel alloy C70600 has good resistance to biofouling, crevice corrosion and stress corrosion cracking, and thus often used as seawater piping material, but it is sensitive to erosion corrosion and galvanic corrosion [7]. Titanium or titanium alloys is very expensive, and aluminum alloy cannot be used at higher temperature and has poor ability of anti-fouling in seawater [8-9]. The higher alloyed 904L, S31254 super austenitic stainless steel, especially the duplex grade S32205 and super duplex S32750 as ideal alternative materials with higher mechanical strength and corrosion resistance to seawater is being applied as high pressure pump, pipeline and etc [10].

Lots of literatures mainly focuses on the corrosion behavior of carbon steel, low alloy steel, 316L, 304 and super ferrite stainless steel in the seawater environment, indicating the main factors of seawater corrosion is attributed to seawater temperature, chloride ion concentration, dissolved oxygen concentration, pH value and microorganism[11-17]. Some conclusions have been obtained that increasing the chloride ion concentration and temperature results in shortening the pregnancy time of pitting, increasing the sensitivity of pitting the and decreasing the pitting potential. Different from the previous literature, concentrated seawater in the LT-MED system is composed of high content multi-component. Recently, S.S. Xin investigated the effect of temperature and concentration ratio on pitting resistance of 316L stainless steel in seawater [18]. The results showed that pitting potential and repassivation potential of the steel all decreased linearly with the logarithm of the concentration rate of seawater in the range of 25 to 95°C and the temperature in the concentration ratio range of 1 to 3 times for seawater, respectively. Few reports on the effect of temperature and seawater concentration simulating the seawater desalinating environment on the pitting corrosion behavior of super duplex stainless steel S32750 could be found.

The main aim of this work is to investigate the effect of seawater temperature and concentration on the electrochemical behavior and semiconducting properties of the passive films formed on the super duplex stainless steel S32750 in LT-MED environment with different seawater concentration and temperatures.

2. EXPERIMENTAL

2.1 Material and test preparation

The super duplex stainless steel S32750 hot rolled plate with 5mm thickness was supplied by TISCO. The chemical composition was shown in Table 1. The specimens of 10.1mm×10.1mm were machined from the hot rolled plate, and then were solution annealed at 1080 ℃ for 1h followed by water quenching. The specimens were wet ground with SiC papers subsequently to 2000 grits. The passivation treatments of the specimens were performed in 20-30 wt% nitric acid solution at 50℃ for 1h to prevent the occurrence of crevice corrosion at high temperature. The work electrodes were mounted in an epoxy resin with exposed area of 1 cm^2 and polished with SiC paper from 200 to 2000 grits.

Table 1. Chemical composition of super duplex stainless steel S32750 (wt%)

Steel	C	Cr	Ni	Mo	N	Si	Mn	P	S	Cu	Fe
S32750	0.018	25.02	7.02	3.94	0.28	0.70	0.93	0.029	0.0005	0.07	Bal.

Three samples of seawater (sample 1, sample 2 and sample 3, corresponding to artificial seawater with 1, 1.5 and 2 times concentration, respectively) were selected as electrolyte for simulating the LT-MED environment. The chemical composition of sample 1 is shown in Table 2 according to ASTM D1141-98 standard, which were prepared by the analytical-grade reagents and triple distilled water. All the tests were performed at 30℃, 50℃ and 70℃, respectively. The experiment temperatures were accurately controlled using the super thermostatic water bath HH-601.

Table 2. Chemical composition of 1 time artificial seawater ($g \cdot L^{-1}$)

	NaCl	$MgCl_2$	Na_2SO_4	$CaCl_2$	KCl	$NaHCO_3$	KBr	H_3BO_3	$SrCl_2$	NaF
Sample 1	24.53	5.20	4.09	1.16	0.695	0.201	0.101	0.027	0.025	0.003
Sample 2	36.795	7.80	6.135	1.74	1.0425	0.3015	0.1515	0.0405	0.0375	0.0045
Sample 3	49.06	10.4	8.18	2.32	1.39	0.402	0.202	0.054	0.05	0.006

2.2 Electrochemical measurements

The potentiodynamic polarization, potentiostatic polarization, cyclic polarization and Mott-Schottky measurements were carried out using a potentiostat PARSTAT 2273, and the Gamry Reference600 system was used for electrochemical impedance spectroscopy (EIS) measurement. The conventional three-electrode cell was utilized for all the experiments. The S32750 stainless steel specimen was the working electrode, and a platinum foil and a saturated calomel electrode (SCE) were used as the counter and reference electrodes, respectively. Electrochemical measurements were started after stabilizating the electrode system for half an hour at open circuit potential.

The potentiodynamic polarization was carried out under different temperature and artificial seawater concentration from the -0.2V below OCP with a scan rate of 0.1667 $mV \cdot s^{-1}$ to obtain the corrosion potential, the pitting potential and passive current density. Prior to the potentiostatic polarization measurements, the working electrode was initially kept potentiostatically at -1.0 V_{SCE} for 600s to remove the air-formed oxide on the surface. The potentiostatic polarization measurements were kept at a passive potential for evaluating the effect of test temperature and artificial seawater concentration on the pitting incubation period. For further understanding the pitting susceptibility of the S32750 steel, the cyclic polarization curves were carried out at a scan rate 0.5 $mV \cdot s^{-1}$ from -0.2 V below OCP. When the current density reached 1mA cm^{-2}, the potential scan was reversed to OCP. The EIS measurements were carried out in the frequency range from 100 kHz to 0.01 Hz with voltage amplitude of 10 mV. The capacitance measurements of passive films were carried out at a fixed frequency 1000Hz at 5 mV amplitude voltage in the potential range -1.0 to 0.5 V_{SCE} by 40 mV steps.

3. RESULTS & DISCUSSION

3.1 Effect of temperature and concentration on the potentiodynamic polarization

Fig.1 shows the potentiodynamic polarization curves of super duplex stainless steel S32750 in sample 3 at 30℃, 50℃ and 70℃. Electrochemical parameters of potentiodynamic polarization in seawater at different temperatures are obtained by the anodic and cathodic regions of the tafel plots shown in Table 3. The corrosion current density (i_{corr}) can be obtained by extrapolating the tafel lines to the corrosion potential. With increasing of the temperature, the values of β_a, β_c and i_{corr} were shifted to higher values. As it can be seen, the temperature exhibits an obvious effect on the corrosion behavior of the S32750. With increasing the temperature, the pitting corrosion potential decreases and the passivity current density increases. The existence of the self-passivation behavior for S32750 can be obviously observed at all temperatures, which indicates that the passive film presents a bilayer structure: an inner layer rich in Cr_2O_3 and an outer porous layer rich in $Cr(OH)_3$[19].

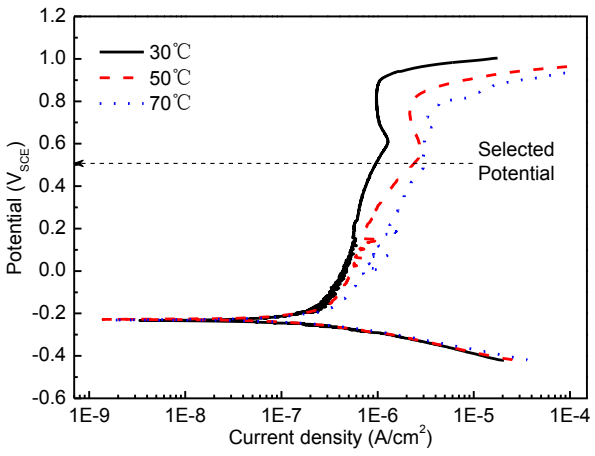

Figure 1. Potentiodynamic polarization curves of S32750 in sample 3 at different temperatures

Moreover, the secondary passivation was observed above 0.5 V_{SCE} at 30℃ and 50℃, which may be associated with the reaction of Cr_2O_3 +5H_2O= 2CrO_4^{2-} + 10H^+ +6e [20]. The presence of Cr^{6+} ion may play an important role in the improved stability of passive films[21], and which improves the pitting corrosion resistance at 30℃ and 50℃. Increasing the temperature to 70℃, the secondary passivation cannot be obviously observed, which may be attributed to the decreasing concentration of dissolved oxygen and oxygen reduction rate and decreasing of the pH values in some localized micro-regions[14], which prevents the formation Cr^{6+}. In addition to increasing temperature, the activity of chloride ions in seawater increase, its collision probability with passive film increases, and the chloride ions excludes the oxygen and combines the metal cations of passive film which promotes the metal dissolution and decreases the corrosion resistance [15].

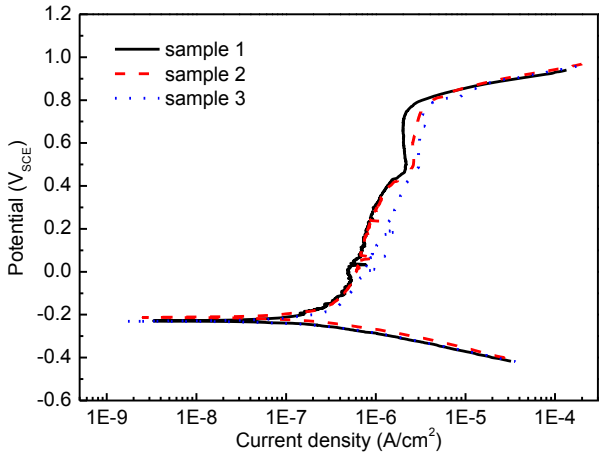

Figure 2. Potentiodynamic polarization curves of S32750 in seawater with different concentration at 70℃

Fig.2 gives the potentiodynamic polarization curves of S32750 in seawater with different concentration seawater at 70℃. The values of β_a, β_c and i_{corr} increased with increasing seawater concentration as shown in Table 3. With increasing seawater concentration, the passivity current density increases and the deceasing of the pitting potential is not notable, indicating that the S32750 has excellent pitting corrosion resistance in high chloride ions concentration at 70℃. The pitting potentials of S32750 are all above 0.8 V_{SCE}, which are higher than those of 316L stainless steel usually used in LT-MED environment the due to higher Cr, Mo, N element content [18]. Higher Cr, Mo, N element may improve the enrichment of nitrogen and the stability of the passive film, and the synergistic effects of molybdenum and nitrogen may furthermore promote the reaction of the formation of the ammonium ions to raise the local pH and facilitate repassivation [22].

Table 3. Electrochemical parameters of potentiodynamic polarization in seawater at different temperatures

Temperature(℃)	Sample	E_{corr}(V_{SCE})	$E_{b,10}$(V_{SCE})	β_a(V)	β_c(V)	i_{corr}(μA·cm^{-2})
30	3	-0.233	0.991	0.276	0.080	0.1504

50	3	-0.228	0.907	0.303	0.085	0.1766
70	3	-0.231	0.833	0.335	0.084	0.2316
70	2	-0.213	0.792	0.310	0.085	0.2129
70	1	-0.228	0.800	0.281	0.082	0.1695

3.2 Effect of temperature and concentration on the incubation period of pitting corrosion

The current-time transients of S32750 obtained in sample 3 at different temperature and in sample 1, sample 2 and sample 3 at 70℃ are shown in Fig.3 and Fig.4, respectively. The values of current density in the transient give the total current resulting from the passive film formation and dissolution of S32750 super duplex stainless steel in the present solution. It is observed that the current density initially decreases rapidly with time at all temperatures and concentrations. This is attributed to the nucleation and growth of the passive film at a rate higher than that of stainless steel dissolution. The current-time transients in sample 3 at 30℃ and 50℃ exhibit that further increment of time results in a relatively steady state current density (i_{ss}) due to the formation of passive film on the surface of S32750 during the entire measurement periods. The current-time transients in sample 1 and sample 2 at 70℃ are also observed that there is a relatively steady state current density (i_{ss}) further increase in time as shown in Fig.4(a). And in sample 3 at 70℃, further increase in time results in the a obvious increase in current density to a relatively high level as shown in the enlargement of Fig.3(a) and Fig.4(a), and this is ascribed to pitting nucleation or steady pitting corrosion [23-24]. The i_{ss} is observed to increase with increasing temperature and concentration in Table 4, indicating that decrease in protective ability of passive film.

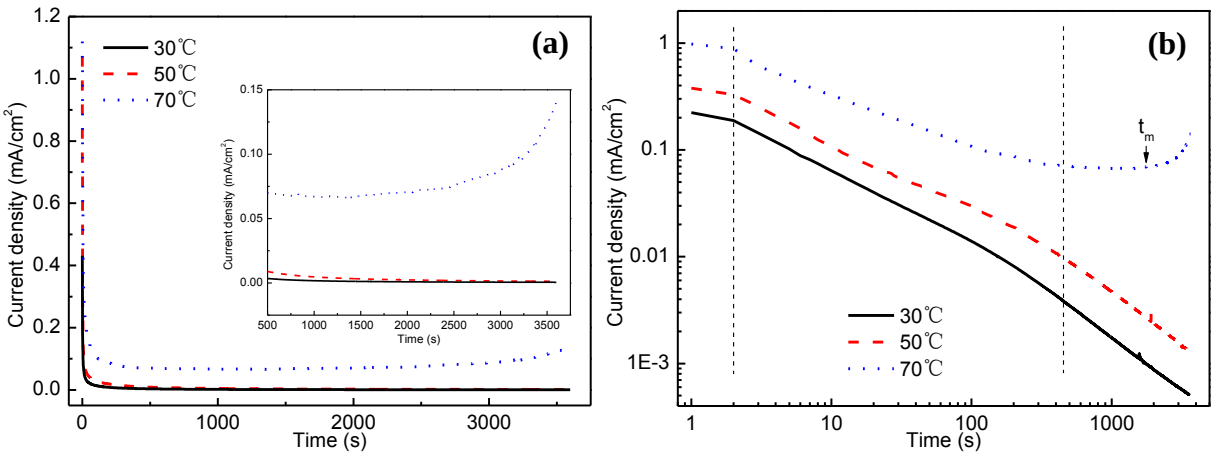

Figure 3. Potentiostatic polarization curves of S32750 in sample 3 at different temperature: (a) Current-time transients; (b) *logi-logt* plots

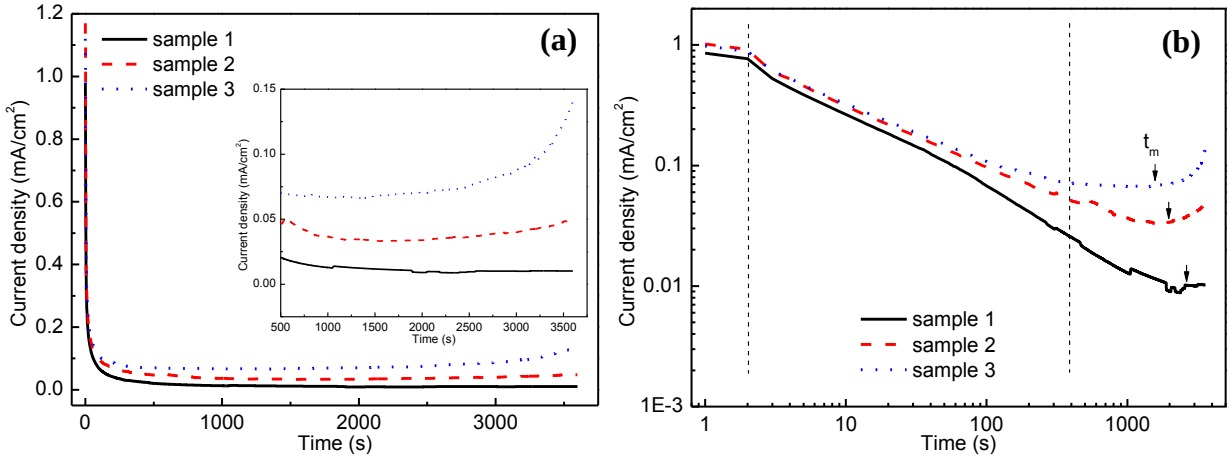

Figure 4. Potentiostatic polarization curves of S32750 in seawater with different concentration at 70℃: (a) Current-time transients; (b) *logi-logt* plots

Fig.3(b) and Fig.4(b) show the log *i* - log *t* plots for S32750 in sample 3 at different temperatures and in the different concentration seawater at 70℃, respectively. Depending on the slope of the curve, it can be divided into three stages, which agrees with other reports about stainless steels [25-27]. The current density for all curves basically keeps constant in the first stage indicating the dynamic equilibrium between film dissolution and growth so that the passive film hardly grows. It is obviously observed that the current density decreases with increasing time belonging to transition period in the second stage. In the third, there are different phenomena found that the current density decreases with time in the logatithmica scale in sample 3 at 30℃ and 50℃, which is ascribed to the formation dense passive film presenting the dissolution of metal [28-29]. But increasing temperature to 70℃ with the range of concentration from 1 to 2 times, the curves exhibit a clear rising after the induction period (t_m) indicating the passive film breakdown due to the growth of pits below pitting potential. From arrowed representation in Fig.3(b) and Fig.4(b), a conclusion can be obtained that the induction period decreases with increasing temperature or concentration of seawater, which means that the temperature and concentration of seawater all exhibit a negative effect on protective ability of passive film for S32750 in LT-MED environment.

The current- time relationship can be described by the following equation.

$$i = At^{-n} \qquad (1)$$

Where *i* represent the current density, A is a constant, *t* is time and n is passivation index. The *n* is a constant value for a given material in a certain environment. All the parameters can be obtained from the linear region slope of log *i* - log *t* curves, which have be considered as an indirect measurement of the formation rate of passive film [28]. It has been reported that n =1 indicates the formation a compact, highly protective passive film, while n = 0.5 indicates the presence of a porous film [30]. The *n* can be obtained based on the equation (1) at different temperatures and in different concentration seawater as listed in Table 4. The value of *n* decreases with increasing temperature and the concentration seawater respectively, indicating the protective property of passive film decreases and the passive film grows slowly with temperature. The values of *n* are found to be between 0.66 and

0.59 in sample 3 at the range of 30℃ to 50℃ and between 0.55 and 0.51 in different concentration seawater at 70℃, indicating that the passive films partially breakdown, and n=0.48 at 70 ℃ in sample 3 indicates the formation of very porous film growing as a result of a dissolution and precipitation process.

Table 4. Electrochemical parameters of potentiostatic polarization in seawater at different temperatures

Temperature(℃)	Sample	i_{ss}(mA·cm^{-2})	n
30	3	5.28×10^{-4}	0.6610
50	3	1.37×10^{-2}	0.5889
70	3	1.18×10^{-1}	0.4790
70	2	4.63×10^{-2}	0.5118
70	1	1.02×10^{-3}	0.5483

From the above experimental results, a conclusion can be obtained that the temperature and concentration have an effect on the stability of passive film formed on S32750 in LT-MED environment. The temperature effectively induces passive film breakdown, which can be interpreted that the movement of the cations and anions becomes easier through passive film with increasing temperature and Cl^- ions, furthermore hinder OH^- or O^{2-} adsorption for the formation of steady passive film. At the same time, the passive current density as the key control step of whole corrosion process is closely related to the protective property of passive film during passivation process [26]. In this case, higher temperature increases the ion conductivity resulting in higher passive current density and deteriorated passive film observed in this work. With increasing the concentration of seawater, more Cl^- ions have opportunity to be adsorbed on the bare metal surface and block the absorption of oxygen ions, which indicates that the dissolution of metal is accelerated and the protective property of passive film is weakened.

3.3 Effect of temperature and concentration on pitting susceptibility

Fig.5 presents the cyclic polarization curves of S32750 in sample 3 at different temperatures. The current density rapidly increases when the potential is rised to transpassive zone, which indicates pits occurring. The pitting potential $E_{b,100}$ decrease with increasing temperature in agreement with the potentiodynamic polarization results. The reverse scan starts at 1mA/cm^2, and the backward scan current densities are lower than forwards at the same potential, indicating that the pits appear and the passive film is difficult to repair. In the reverse scan, the current density continues to increase to a hump value i_{max}. The i_{max} increases with increasing temperature which is attributed to the self-catalytic effect of the pits formed in the forward scan, resulting in continuous development of pits. Even if reverse scan is carried out, the pits development can not be hindered. With further decreasing the potential, the reverse scan current density greatly decreases and intersects with the forward scan, where the repassivation potential or protection potential E_p reached indicating that below which the active

pits repassivate and existing pits no longer grow[31-32]. The E_p values increase with increasing the solution temperature which denotes that the repair ability of existing pits decrease. The potential difference, E_b - E_p defined as the imperfect passivity zone, is a measure of the trend of nucleated pitting growth [33]. Intermediates values between E_b and E_p do not permit the formation of new pits, but allow the development of the existing ones [31, 34-35]. The E_b - E_p values increase with increasing solution temperature indicating increased pitting susceptibility. The existence of the hysteresis loop in cyclic potentiodynamic polarization curve indicates that repassivation of an existing pit is more difficult when the potential scans toward the negative direction. The area of hysteresis loop of the S32750 in sample 3 with increasing the temperature from 30℃ to 70℃ becomes larger as shown Fig.5 and Table 5, which indicates that the extent of damage of the passive film increases, self-repairing ability of the passive film is weakened and pitting susceptibility increases at higher temperature.

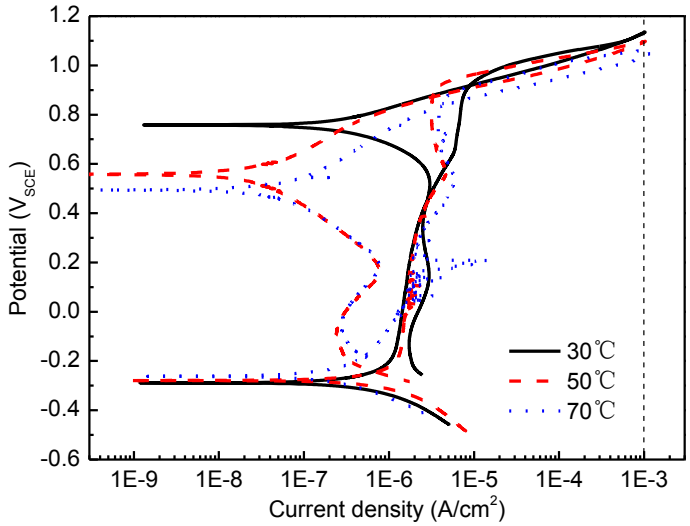

Figure 5. Cyclic polarization curves of S32750 in sample 3 at different temperature

The cyclic polarization curves of S32750 in seawater with different concentration at 70℃ are shown in Fig.6. With increasing the seawater concentration from 1 to 2 times, the pitting potential $E_{b,100}$ deceases. The result is attributed to the probability of Cl^- colliding on the oxide film with rising Cl^- concentration. Furthermore, more Cl^- has more opportunities combined with cation to form the soluble halide which can accelerate the occurrence of pitting corrosion. The protection potential Ep decreasing with increasing seawater concentration as shown Table 5 indicates that the repair ability of existing pits decrease at higher seawater concentration. It is also observed in the Table 5 that ($E_b - E_p$) difference and the area of hysteresis loop become larger with higher seawater concentration, which is interpreted that the repair of passive films formed on the S32750 decease with increasing the seawater concentration, and the pitting susceptibility of passive films increase.

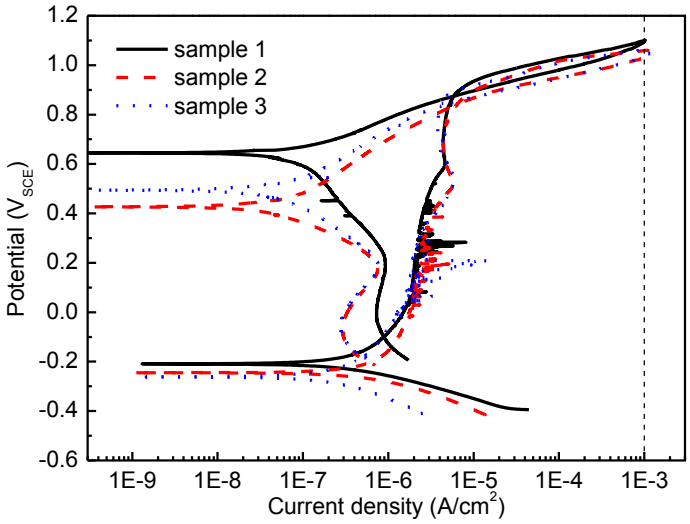

Figure 6. Cyclic polarization curves of S32750 in seawater with different concentration at 70℃

Table 5. Cyclic polarization parameters of in seawater at different temperatures

Temperature(℃)	Sample	$E_{b,100}$(V_{SCE})	E_p(V_{SCE})	$E_{b,100}$-E_p(V)	i_{max}(mA·cm^{-2})
30	3	1.047	0.918	0.129	1.03
50	3	1.028	0.872	0.156	1.04
70	3	1.009	0.833	0.176	1.19
70	2	1.017	0.848	0.169	1.25
70	1	1.027	0.878	0.149	1.03

3.4 Effect of temperature and concentration on impedance of passive films

For a better understanding of the effect of temperature and seawater concentration on the corrosion behavior of S32750 in LT-MED environment, the electrochemical impedance spectroscopy tests were performed in seawater with different temperature and seawater concentration, respectively. Bode plots obtained in sample 3 with the temperature of 30 ℃, 50℃ and 70℃ are shown in Fig.7. In the extremely high-frequency region, impedance modulus values reflect the solution resistance Rs [14, 25], the increasing of temperature results in reducing of the solution viscosity, and the diffusion rate can be increased to accelerate the dissolution of the passivation film and ion diffusion, resulting in the decreasing of water resistance [36]. In the very low-frequency region, the impedance modulus values represent the electrode polarization resistance. With increasing temperature, the polarization impedance of super duplex stainless steel S32750 decreases, indicating that the stability of the passive film deteriorates, and the corrosion rate increases.

Two peaks in the phase angle plot are clearly observed as shown in Fig.7(b), corresponding to two relaxation time constants. This indicates and confirms that the passive films formed on the S32750 in the temperature range from 30℃ to 70℃ have a bilayer structure[19]. In all temperature range, the phase angles are all lower than 90°indicating that the behavior can be interpreted as a deviation from ideal capacitor behavior[37-39]. On this basis, the use of a constant phase element CPE is necessary

[40-41] due to a distribution of relaxation times resulting from surface heterogeneities, adsorption of species, and the formation of porous layers. The impedance of the CPE is given by:

$$Z_{CPE} = \frac{1}{Q}(j\omega)^{-n} \qquad (2)$$

Where Q is the CPE constant, ω the angular frequency(rad/s), j^2=-1 the imaginary number and n is the CPE exponent.

The impedance spectra of S32750 in sample 3 with different temperatures were well fitted by equivalent circuit $R_{sol}\{Q_1[R_1(Q_2R_2)]\}$. Fitted parameters are listed in Table 6. The total impedance is:

$$Z_{total} = R_{sol} + \left(Q_1(j\omega)^{n_1} + \frac{1 + R_2Q_2(j\omega)^{n_2}}{R_1 + R_2 + R_1R_2(j\omega)^{n_2}} \right)^{-1} \qquad (3)$$

Where R_{sol} represents the electrolyte resistance, R_1 is the outer porous film resistance, Q_1 is double layer capacitance, R_2 is inner passive film resistance and Q_2 is the capacitance of the passive film formed as an inner layer on the S32750.

According to the fitting parameters shown in Table 6, the inner passive film resistance R_2 is greater than the outer porous film resistance R_1, which represents the protection of S32750 is provided by the inner oxide layer, while the outer film is more defective [42]. R_2 decreases with increasing temperature, indicating that the conductivity increases and the inner oxide layer dissolves and becomes thinner [42], and the corrosion resistance of the steel decreases.

Fig.8 shows the Bode plots obtained in sample 1, sample 2 and sample 3 at 70℃. The impedance modulus values in the extremely high-frequency and low-frequency region all decrease with increasing the seawater concentration from 1 times to 2 times as shown Fig.8(a), which indicates that the stability of the passive film decreases and the corrosion rate of the steel increases.

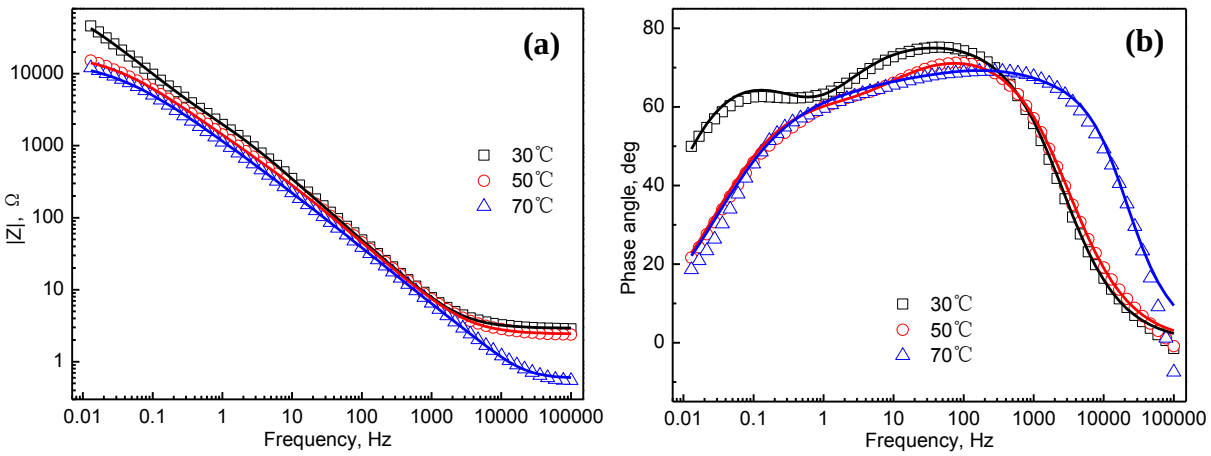

Figure 7. Bode plots of S32750 in sample 3 at different temperatures: (a) Impedance modulus; (b)Phase angle

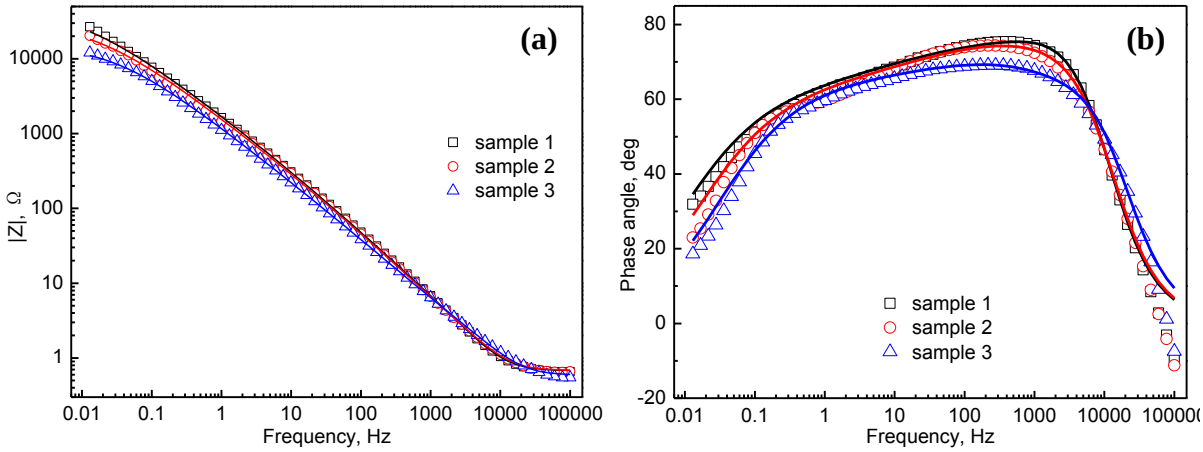

Figure 8. Bode plots of S32750 in seawater with different concentration at 70℃: (a) Impedance modulus; (b) Phase angle

There are also two relaxation time constants of the phase angle plot and which are all lower than 90°(Fig.8(b)). Fitting parameters using the same equivalent circuit $R_{sol}\{Q_1[R_1(Q_2R_2)]\}$ are also listed in Table 6 for considering the effect of seawater concentration. The inner passive film resistance R_2 is also much greater than the outer porous film resistance R_1. R_1 and R_2 all slightly decrease with increasing concentration of seawater, indicating that increasing seawater concentration promotes the dissolution of passive film formed on the S32750.

Table 6. Fitting results of the equivalent circuit of S32750 in seawater at different temperatures

Temperature(℃)	Sample	R_{sol}	Q_1	n_1	R_1	Q_2	n_2	R_2
30	3	2.907	7.837×10^{-5}	0.8648	4447	7.802×10^{-5}	0.7912	9.692×10^{4}
50	3	2.408	9.54×10^{-5}	0.8441	1094	1.111×10^{-4}	0.6372	1.826×10^{4}
70	3	0.5926	1.605×10^{-5}	1	4.02	2.096×10^{-4}	0.6881	1.503×10^{4}
70	2	0.6834	1.963×10^{-5}	1	7.488	1.543×10^{-4}	0.6643	2.971×10^{4}
70	1	0.6797	2.102×10^{-5}	1	16.96	1.398×10^{-4}	0.6601	4.514×10^{4}

3.5 Effect of temperature and concentration on semiconducting properties of passive films

The semiconducting properties of passive films formed on S32750 in different temperature and concentration seawater could be obtained from capacitance measurements. The relationship between capacitance and applied potential is given by the well-known Mott-Schottky (MS) equation [23, 43-44].

$$\frac{1}{C^2} = \frac{2}{\varepsilon\varepsilon_0 e N_D}\left(E - E_{fb} - \frac{kT}{e}\right) \quad \text{for n-type semiconductor} \qquad (4)$$

$$\frac{1}{C^2} = -\frac{2}{\varepsilon\varepsilon_0 e N_A}\left(E - E_{fb} - \frac{kT}{e}\right) \quad \text{for p-type semiconductor} \qquad (5)$$

Where C is the space charge capacitance, ε is the dielectric constant of the passive film(15.6), ε_0 is the permittivity of free space (8.854×10^{-14}F/cm), e is the electron charge(1.602×10-19C), N_D and N_A are the donor and acceptor densities, respectively. E_{fb} is the flat band potential, k is the Boltzmann constant (1.38×10-23J/K), and T is the absolute temperature. N_D and N_A can be determined from the slope of the experimental $1/C^2$ vs. applied potential (E).

Fig.9 and Fig.10 show the Mott-Schottky plots of S32750 stainless steel in sample 3 at different temperatures (30, 50 and 70℃) and in sample 1, sample 2 and sample 3 at 70℃, respectively. Firstly, it is all clearly noted that capacitance increases with temperature and seawater concentration. Secondly, the existence of three linear regions (R1, R3 and R4) between C^{-2} and E and a narrow potential plateau region (R2) is obviously observed.

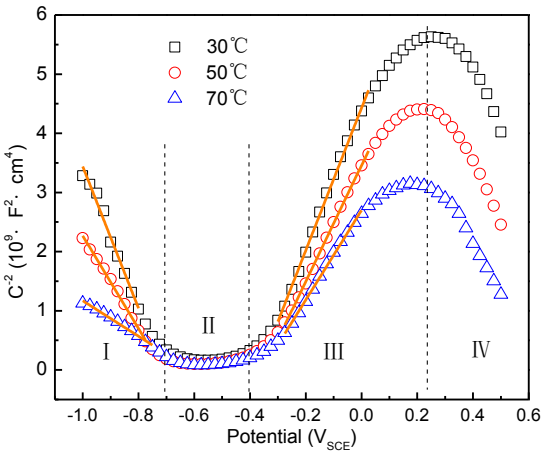

Figure. 9 Mott-Schottky plots of S32750 in sample 3 at different temperature

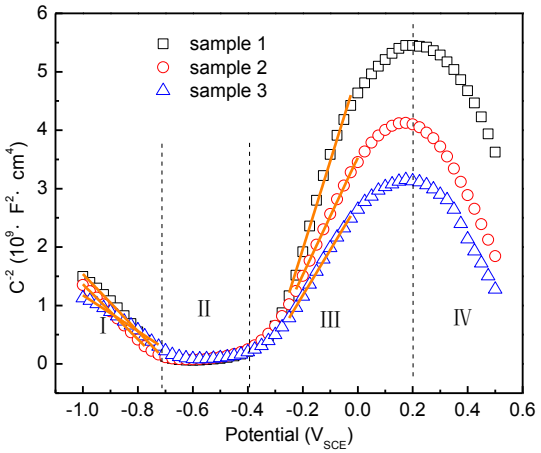

Figure. 10 Mott-Schottky plots of S32750 in seawater with different concentration at 70℃

The negative slopes in R1 region present a p-type semiconductor that is related to the inner chromium-rich layer of the passive film on stainless steel. The positive slopes above R2 region behave

an n-type semiconductor that is attributed to the outer porous iron-rich layer[45]. The capacitance results show the fact that the passive films had a duplex character. Finally, the negative slopes in the R4 above $0.2V_{SCE}$ are also typical semiconductor, which is possibly explained in terms of a strong dependence of Faradaic current on potential in the transpassive region [46]. In this sense, the behavior of capacitance at high potentials near the transpassive region is attributed to development of an inversion layer due to an increasing concentration in the valence band (high valency Cr in the film prior to transpassive dissolution).

According to Mott-Schottky equation (4) and (5), the donor (N_D) and acceptor (N_A) densities could be calculated from the slopes of the linear regions R1 and R3 in Fig.9 and Fig.10. Table 7 shows the N_D and N_A values for films formed on S32750 in sample 3 at different temperatures and in seawater with different concentration at 70℃. The doping densities values are all in the range of 10^{20}-10^{21}cm^{-3}, which agree well with the values by other researchers [43-46]. From Table 7, it can be clearly seen that the donor and acceptor densities increase at higher seawater temperature and concentration. High doping densities indicate the highly disordered character of passive films [47], which represents that both the outer and inner layers of passive films formed on S32750 become more defective with increasing seawater temperature and concentration. At the same time, acceptor and donor has been reported to increase with increase in conductivity of passive film, which implies that higher acceptor or donor density with increasing seawater temperature and concentration will lead to high values of the passive current density. The results are consistent with the potentiodynamic polarization and current-time transient curves. All these statements confirm the protective ability of the passive films formed on S32750 decreases with increasing seawater temperature and concentration in the LT-MED environment. The chloride ions effect can be related to the PDM [48]. Chloride ion can be absorbed into the film/solution interface and react with oxygen vacancy via a Mott–Schottky pair type of reaction to generate cation/oxygen vacancy pairs. The oxygen vacancies in turn, react with the additional chloride ions at the film/solution interface to generate more cation vacancies. Therefore, the generating of cation/oxygen vacancy is autocatalytic, the excess vacancies arrive at the metal/film interface and condense, and then lead to local detachment of the film from underlying metal. The chloride ion concentration increases with increasing the seawater concentration, and the passive film has more doping densities which is always associated with lower pitting corrosion resistance. The effect of temperature on acceptor or donor densities of passive films can be interpreted that higher temperature promotes electrolyte solubility and make mass transport easier due to convection[19], more generating of cation/oxygen vacancy is related to the acceptor or donor densities increasing. Therefore, the pitting corrosion resistance of S32750 decreased with increasing seawater temperature and concentration.

Table 7. Donor and acceptor densities of the passive film formed on Super Duplex Stainless steel S32750 in seawater at temperatures between 30 and 70 ℃

Temperature(℃)	Sample	N_A (cm^{-3})	N_D(cm^{-3})
30	3	8.24×10^{20}	7.52×10^{20}
50	3	1.16×10^{21}	9.23×10^{20}

70	3	2.91×10^{21}	1.17×10^{21}
70	2	1.93×10^{21}	8.77×10^{20}
70	1	1.85×10^{21}	6.02×10^{20}

4. CONCLUSION

From the results of present instigation the following conclusions can be drawn on the effects of temperature and seawater concentration on electrochemical characteristics of super duplex stainless steel S32750 in LT-MED environment:

(1) The potentiodynamic polarization curves and potentiostatic polarization curves show the pitting corrosion potential decreases, the passivity current density increases and induction period of pitting shortens with the increase of temperature and seawater concentration. The passivation index *n* decreases with increasing temperature and the concentration seawater respectively, indicating the protective property of passive film decreases and the passive film grows slowly with temperature.

(2) The cyclic polarization curves reveal that E_b - E_p values and the area of hysteresis loop become larger with higher temperature and seawater concentration, which is interpreted that the repair of passive films formed on the S32750 decease with increasing the temperature and seawater concentration, and the pitting susceptibility of passive films increase.

(3) EIS analysis indicates that impedance decreases with increasing temperature and seawater concentration, and the protection of S32750 is provided by the inner oxide layer, while the outer film is more defective.

(4) Mott-Schottky analysis shows that passive film formed on S32750 present bilayer structure, and behaves as n-type and p-type, respectively. The donor and acceptor densities increase with seawater temperature and concentration, which indicates that passive films become more defective, resulting in decreasing of protective ability of the passive films.

ACKNOWLEDGEMENTS
The present research was financially supported by National Key Technology Research and Development Program of the Ministry of Science and Technology of China(No. 2012BAE04B01), National Natural Science Foundation of China(No.51304041), China Postdoctoral Science Foundation(No. 2013M530936) and Program for New Century Excellent Talents in University(No. N130502001).

Reference

1. A. D. Khawajia, I. K. Kutubkhanah, J.M. Wie, *Desalination*, 221 (2008) 47
2. K. L. Yu, Q. C. Lv, G. L. Ruan, *China Water & Wastewater,* 24 (2008) 81
3. B. K. Sun, N. Li, M.Du, *Mater. Protection*, 44(2011)20
4. P. Budhiraja, A. A. Fares, *Desalination*, 220(2008)313
5. M. Al-Shammiri, M. Safar, *Desalination*, 126(1999)45
6. S. S. Xin, M. C. Li, J. N. Shen, *Acta Metall. Sin.*, 50(2014)373
7. H. I. Al Hossani, T.M.H. Saber, R.A. Mohammed, A.M. Shams El Din, *Desalination*, 109(1997)25
8. H. Ezuber, A. El-Houd, F. El-Shawesh, *Mater. Des.*, 29(2008) 801.
9. X. Q. Meng, Z. Y. Lin, F. F. Wang, *Mater. Des.*, 51(2013) 683

10. A. M. Hassan, A.U. Malik, *Desalination*, 74 (1989) 157
11. H. T. Wan, *Corrosion & Protection*, 26(2005)373.
12. K. S. E. Al-Malahy, T. Hodgkiess, *Desalination*, 158(2003)35
13. S. J. Yuan, S. O. Pehlconen, *Corros.Sci.*, 57(2009)7372
14. X. Wei, J. H. Dong, J. Tong, Z. Zheng, W. Ke, *Int. J. Electrochem.*, 8(2013)887
15. X. Wei, J. H. Dong, J. Tong, Z. Zheng, W. Ke, *Acta Metall. Sin.*, *4*8(2012)502
16. J. O. Park, S. Matsch, H. Böhni, *J. Electrochem. Soc.*, 149(2002) B34
17. A. U. Malik, P. C. Mayan Kutty, N. A. Siddiqi, I. N. Andijani, S. Ahmed, *Corros.Sci.*, 33(1992)1809
18. S. S. Xin, M. C. Li, *Corros.Sci.*, 87(2014)96
19. M. V. Cardoso, S. T. Amaral, E. M. A. Martini, *Corros.Sci.*, 50(2008)2429
20. M. Gojic, D. Marijan, L. Kosec, Corrosion, 56(2000)839
21. J. B. Lee, S. W. Kim. *Mater. Chem. Phys.*, 104 (2007)98
22. H. B. Li, Z. H. Jiang, Y. Yang, Y. Cao, Z. R. Zhang, *Int. J. Min. Met. Mater.*, 16(2009)517
23. Y. X. Qiao, Y. G. Zheng , W. Ke, P.C. Okafor, *Corros.Sci.*, 51 (2009) 979
24. G. O. Ilevbare , G. T. Burstein, *Corros.Sci.*, 43 (2001) 485
25. C. Escriva-Cerdan, E. Blasco-Tamarit, D. M. Garcia-Garcia, J. Garcia-Anton, R. Akid , J. Walton , *Electrochim. Acta.*, 111(2013) 552
26. J. B. Lee, *Mater. Chem. Phys.*, 99(2006),224
27. R. M. Fernandez-Domene, E. Blasco-Tamarit, D. M. Garcia-Garcia, J. Garcia–Anton, *Corros.Sci.*, 52(2010)3453
28. J. Kim, S. Pyun, *Electrochim. Acta.*, 40(1995)1863
29. S. Pyun, E. Lee, *Electrochim. Acta.*, 40(1995)1963
30. J. R. Galvele, R. M. Torresi, R. M. Carranza, *Corros.Sci.*, 31(1990)563
31. Y. Y. Chen, L. B. Chou, H. C. Shih, *Mater. Sci. Eng., A*, 396(2005)129
32. A. Igual Muñoz, J. García Antón, J.L. Guiñón, V. Pérez Herranz, *Corros.Sci.*, 48(2006)3349–3374.
33. T. Bezelle, G. Roventi, R. Fratesi, *Electrochim. Acta*, 49 (2004) 3005
34. B. E. Wilde, *Corrosion*, 28(1972)283
35. A. Pardo, E. Otero, M. C. Merino, M. V. Utrilla, F. Moreno, *Corrosion*, 56(2000)411
36. C. F. Dong, H. Luo, K. Xiao, T. Sun, Q. Liu, X. G. Li, *J. WuHan. Univ. Technol.*, 26(2011)641
37. Y. Fu, X. Q. Wu, E.H. Han, W. Ke, K. Yang, Z.H. Jiang, *Electrochim. Acta*, 2009, 54(2009)1618
38. A. Carnot, I. Frateur, S. Zanna, B. Tribollet, I. Dubois-Brugger, P. Marcus, *Corros.Sci.*,45(2003)2513
39. C. Hitz. A. Lasia, *J. Electroanal. Chem.*, 500(2001) 213
40. G. J. Brug, A. L. G. Vandeneeden, M. Sluytersrehbach, J. H. Sluyters, *J. Electroanal. Chem.*, 176(1984)275
41. F. B. Growcock, J. H. Jasinski, *J. Electrochem. Soc*., 1989, 136: 2310.
42. C. Escriva-Cerdan, E. Blasco-Tamarit, D. M. Garcia-Garcia, J. García-Antóna, A. Guenbour, *Electrochim. Acta*, 80(2012) 248
43. A. Di Paola, *Electrochim. Acta*, 34(1989)203
44. Y. Fu, X.Q. Wu, E. H. Han, W. Ke, K. Yang, Z. H. Jiang, *J. Electrochem. Soc*., 155(2008)455
45. R. A. Antunes, M. C. L. de Oliveria, I. Costa, *Mater. Corro.*,63(2012)586
46. T. L. Sudesh, L. Wijesinghe, D. J. Blackwood, *Corros. Sci.*, 50(2008)94
47. C. Escriva-Cerdan, E. Blasco-Tamarit, D.M. Garcia-Garcia, J. García-Antóna, A. Guenbour, *Electrochim. Acta*, 80(2012)248
48. D. D. MacDonald, *J. Electrochem. Soc.*, 139(1992)3434